3024 *Chem. Mater.* **2010,** *22,* 3024–3032
DOI:10.1021/cm902904u

CHEMISTRY OF MATERIALS
Article

Atomic Layer Deposition (ALD) Co-Deposited Pt−Ru Binary and Pt Skin Catalysts for Concentrated Methanol Oxidation

Xirong Jiang,[†] Turgut M. Gür,[‡] Friedrich B. Prinz,[‡,§] and Stacey F. Bent*[,⊥]

[†]*Department of Physics, Stanford University, Stanford, California 94305,* [‡]*Department of Materials Science and Engineering, Stanford University, Stanford, California 94305,* [§]*Department of Mechanical Engineering, Stanford University, Stanford, California 94305, and* [⊥]*Department of Chemical Engineering, Stanford University, Stanford, California 94305*

Received September 17, 2009. Revised Manuscript Received March 6, 2010

In this study, we demonstrate a novel approach—atomic layer deposition (ALD)—for the synthesis and investigation of Pt−Ru catalyst structures toward the oxidation of stoichiometric (1:1) methanol solutions in advanced direct methanol fuel cells. Two types of thin-film materials are investigated as catalysts for methanol oxidation: Pt−Ru films of varying ruthenium content that are co-deposited by ALD, and Pt skin catalysts made by depositing porous platinum layers of different thickness by ALD on sputtered ruthenium films. $MeCpPtMe_3$ and $Ru(Cp)_2$ are used as precursors for Pt and Ru ALD, respectively, together with pure O_2 as the counter reactant. The electrochemical behavior of the co-deposited Pt−Ru catalysts and the Pt skin catalysts for methanol oxidation is characterized using chronoamperometry and cyclic voltammetry in a 0.5 M H_2SO_4/16.6 M CH_3OH electrolyte at room temperature. The results illustrate that the optimal stoichiometric Pt:Ru ratio for the co-deposited catalysts is ∼1:1, which is consistent with our previous study on sputtered Pt−Ru catalysts using the same CH_3OH concentration. Moreover, we report that the catalytic activity of sputtered ruthenium catalysts toward methanol oxidation is strongly enhanced by the ALD Pt overlayer, with such skin catalysts displaying superior catalytic activity over pure platinum. The mechanistic aspects of our observations are discussed.

Introduction

Over the last several decades, direct methanol fuel cells (DMFCs) have attracted great interest.[1,2] Compared to hydrogen-based fuel cells, DMFCs provide improved logistics of using a liquid fuel with a significantly higher energy density (5 kWh/L for methanol vs 3 kWh/L for hydrogen compressed at 5000 psi). Potentially, this provides energy densities that are 10 times better than that of Li-ion batteries, and it makes DMFCs an attractive power source for portable military and commercial applications.[1−4] However, the current electrocatalysts used in DMFCs require further improvement before DMFCs will become competitive with conventional engine technology.[4] Of the many types of catalysts reported, mixed-metal catalysts that contain platinum are currently favored for methanol oxidation.[5,6] However, the high cost of platinum in such catalysts prevents the practical application of DMFCs on a large scale.[2,5−9]

In this paper, we explore two different strategies to increase the activity and utilization levels of platinum while reducing its loading. One approach is to replace or alloy platinum with other less-expensive materials. Previously, materials including ruthenium, osmium, rhodium, tin, nickel, zirconium, tungsten, iridium, tungsten oxide, and ruthenium oxide have been alloyed with platinum through various methods such as impregnation, colloidal methods, microemulsion, and sputtering, with some reports showing superior activity or stability of these alloys, compared to pure platinum.[5,6,10−21] The originality of the work presented here involves a novel

*Author to whom correspondence should be addressed. Tel.: 001 650 723 0385. Fax: 001 650 723 9780. E-mail address: sbent@stanford.edu.

(1) Icardi, U. A.; Specchia, S.; Fontana, G. J. R.; Saracco, G.; Specchia, V. *J. Power Sources* **2008**, *176*(2), 460.
(2) Thompsett, D.; Hogarth, M. *Fuel Cell Technology Handbook*; CRC Press: Boca Raton, FL, 2003; p 6-1.
(3) O'Hayre, R.; Cha, S.; Colella, W.; Prinz, F. B. *Fuel Cell Fundamentals*; John Wiley and Sons: New York, 2006.
(4) *Fuel Cell Handbook*, 7th ed.; U. S. Department of Energy: Morgantown, WV, 2004; p 3-1.
(5) Beden, B.; Kadirgan, F.; Lamy, C.; Leger, J. M. *J. Electroanal. Chem.* **1981**, *127*(1−3), 75.
(6) Liu, H.; Song, C.; Zhang, L.; Zhang, J.; Wang, H.; Wilkinson, D. P. *J. Power Sources* **2006**, *155*(2), 95.
(7) Yajima, T.; Uchida, H.; Watanabe, M. *J. Phys. Chem. B* **2004**, *108* (8), 2654–2659.
(8) Kua, J.; Goddard, W. A. *J. Am. Chem. Soc.* **1999**, *121*(47), 10928–10941.
(9) Hamnett, A. *Catal. Today* **1997**, *38*(4), 445.
(10) Dubau, L.; Coutanceau, C.; Garnier, E.; Léger, J. M.; Lamy, C. *J. Appl. Electrochem.* **2003**, *33*(5), 419.
(11) Dickinson, A. J.; Carrette, L. P. L.; Collins, J. A.; Friedrich, K. A.; Stimming, U. *J. Appl. Electrochem.* **2004**, *34*(10), 975.
(12) Witham, C. K.; Chun, W.; Valdez, T. I.; Narayanan, S. R. *Electrochem. Solid-State Lett.* **2000**, *3*(11), 497–500.
(13) Guo, J.; Sun, G.; Sun, S.; Yan, S.; Yang, W.; Qi, J.; Yan, Y.; Xin, Q. *J. Power Sources* **2007**, *168*(2), 299.
(14) Guo, J.; Sun, G.; Wu, Z.; Sun, S.; Yan, S.; Cao, L.; Yan, Y.; Su, D.; Xin, Q. *J. Power Sources* **2007**, *172*(2), 666.
(15) Jiang, X.; Prinz, F. B.; Bent, S. F. *Electrochem. Soc. Trans.* **2008**, *16*(2), 605.

 Published on Web 04/21/2010

approach—namely, atomic layer deposition (ALD)—for fabricating Pt−Ru catalysts where the composition of the Pt−Ru catalyst is controlled by changing the ratio of the number of Pt ALD cycles to the number of Ru ALD cycles. Because of the self-limiting reaction mechanism of ALD,[22,23] we are able to achieve precise control of the platinum and ruthenium loading levels.

A second approach that we explore is the fabrication of Pt skin catalysts using ALD. For this type of catalyst, we examine the model case of a bimetallic catalyst consisting of a metal monolayer on another metal surface. Such catalysts have been extensively studied in ultrahigh vacuum[24] and, to a lesser extent, in electrochemical systems.[25] Theoretical work by Mavrikakis et al. and Nørskov et al. has determined that several metal substrates under a platinum overlayer are able to weaken the bond strength between the methanol oxidation intermediates and platinum,[26−28] leading to potentially higher catalytic activity, compared to pure platinum. In this study, we coated sputter-deposited ruthenium films with a layer of platinum using ALD, where the platinum loading is accurately controlled by the number of ALD cycles, because of its self-limiting surface reaction mechanism.[22,23] The motivation is to investigate the impact of a platinum overlayer of various thicknesses on the catalytic activity of sputtered ruthenium films toward methanol oxidation, with the goal of ultimately achieving higher activity with reduced platinum loading. Another motivation and originality of the present work is to study the electrocatalytic behavior of these prospective anode materials in stoichiometric (1:1 molar ratio) methanol−water solutions, where such information is scarce but badly needed for possible development of advanced DMFCs[29,30] whose objective is to eliminate the methanol crossover problem that is commonly observed in hydrated acid polymer membrane cells.[31] This would then allow the use of stoichiometric fuel for internal reforming without a loss in open circuit voltage, conversion efficiency, and fuel utilization.

In this paper, we will first introduce the processes of Pt and Ru ALD, as well as the preparation of the ALD co-deposited Pt−Ru film catalysts and Pt skin catalysts. We then will present the results of the physical and electrochemical studies on each of these catalysts.

Experimental Methods

Sample Preparation. Silicon substrates, cut from Si(100) wafers (*p*-type with a boron dopant; resistivity of 1.0 −10.0 Ω cm, Si-Tech, Inc.) and pretreated in piranha solution, as well as ruthenium films sputtered onto silicon substrates, were used to characterize the ALD processes. Fluorine-doped tin oxide (FTO)-coated glass (Hartford Glass Co., Inc.) was used as a substrate for fabrication of Pt−Ru half-cell catalytic electrodes for the electrochemical measurements. The silicon substrates were cleaned by the piranha solution at room temperature. The piranha solution, which contained a 7:3 ratio of 98% sulfuric acid:30% hydrogen peroxide, was used to prepare a chemical oxide on the silicon substrates. [*Caution: Fresh piranha solution is hot and extremely corrosive. Proper training and extreme care should be taken when handling piranha solution.*] The FTO substrates were sonicated in a 50:50 ethanol−water mixture for 15 min, followed by thorough rinsing in deionized water, sonication in deionized water, and drying in a stream of dry air prior to deposition.

We used a custom-built, warm-wall flow reactor for all ALD processing. The ALD reactor design was previously described and specifications were reported earlier.[32] (Methylcyclopentadienyl)-trimethylplatinum ($MeCpPtMe_3$) (Strem) and bis(cyclopentadienyl)ruthenium ($Ru(Cp)_2$) (Strem) were used as the metal precursors for Pt ALD and Ru ALD, respectively. For both ALD processes, pure oxygen (Praxair) was used as a counter reactant, and nitrogen gas (99.9995%) was used as both a purging gas and a carrier gas. Both platinum and ruthenium thin-film deposition by ALD were initially studied by Aaltonen et al.[33,34] In our process, the $MeCpPtMe_3$ and pure O_2 source temperatures were 65 °C and room temperature (20−25 °C), respectively. A Pt ALD cycle consisted of a 2-s exposure to $MeCpPtMe_3$, a 12-s N_2 purge, a 1-s exposure to O_2, and a 12-s N_2 purge. In the Ru ALD process, the $Ru(Cp)_2$ and pure O_2 source temperatures were 80 °C and room temperature, respectively . The $RuCp_2$ dose time was 2 s, and the N_2 purge time was 12 s after both precursor pulses. The oxygen flow rate in both Ru and Pt ALD processes was kept at 15 sccm. The oxygen pulse time was varied as described in the Results and Discussion section.

For Pt−Ru co-deposition of samples S1−S5 (see Table 1), a procedure involving ALD "super cycles" was used to fabricate the Pt−Ru electrodes of different stoichiometry. For example, in the deposition scheme used for the preparation of sample S4, one super cycle consisted of 4 cycles of Pt ALD, followed by 16 cycles of Ru ALD. Each super cycle was repeated until the total number of individual ALD cycles reached ∼200. Depending on the super cycle, the total film thickness varied over a range of 10.0−13.6 nm. For all of the co-deposition processes, the substrate temperature was kept at 245 °C and a 3-nm-thick platinum film was predeposited as a seed layer by ALD to promote ruthenium nucleation.

To prepare the Pt skin catalysts, ruthenium films 80 nm thick were dc-sputtered onto electrically conducting FTO substrates.

(16) Jiang, X.; Gür, T. M.; Prinz, F. B.; Bent, S. F. *J. Electrochem. Soc.* **2010**, *157*, B314–B319.
(17) Zhang, J.; Vukmirovic, M. B.; Xu, Y.; Mavrikakis, M.; Adzic, R. *Angew. Chem., Int. Ed.* **2005**, *44*(14), 2132.
(18) Bligaard, T.; Nørskov, J. K. *Electrochim. Acta* **2007**, *52*(18), 5512.
(19) Jayaraman, S.; Jaramillo, T. F.; Baeck, S. H.; McFarland, E. W. *J. Phys. Chem. B* **2005**, *109*(48), 22958–22966.
(20) Kawaguchi, T.; Rachi, Y.; Sugimoto, W.; Murakami, Y.; Takasu, Y. *J. Appl. Electrochem.* **2006**, *36*(10), 1117.
(21) Huang, S. F. C.; Y.; Liu, C. S.; Carty, A. J.; Mast, K.; Bock, C.; MacDougall, B.; Peng, S. M.; Lee, G. H *Chem. Vap. Deposition* **2003**, *9*, 157–161.
(22) Ritala, M.; Leskela, M. *Handbook of Thin Film Materials*; Academic Press: New York, 2002; Vol. *1*.
(23) George, S. M. *Chem. Rev.* **2010**, *110*, 111–131.
(24) Rodriguez, J. A. *Surf. Sci. Rep.* **1996**, *24*, 225.
(25) Schmidt, T. J.; Stamenkovic, V.; Arenz, M.; Markovic, N.; Ross, P. N. *Electrochim. Acta* **2002**, *47*, 3765.
(26) Greeley, J.; Mavrikakis, M. *Catal. Today* **2006**, *111*(1−2), 52.
(27) Hammer, B.; Nørskov, J. K. *Adv. Catal.* **2000**, *45*, 71.
(28) Greeley, J.; Nøskov, J. K.; Mavrikakis, M. *Annu. Rev. Phys. Chem.* **2002**, *53*, 319.
(29) Shim, J. H.; Cha, S. W.; O'Hayre, R.; Gur, T. M.; Prinz, F. B. *Electrochem. Soc. Trans.* **2006**, *3*, 1059.
(30) Shim, J. H.; Park, J. S.; An, J.; Gur, T. M.; Kang, S.; Prinz, F. B. *Chem. Mater.* **2009**, *21*(14), 3290–3296.
(31) Wang, Z. H.; Wang, C. Y. *J. Electrochem. Soc.* **2003**, *150*(4), A508–A519.
(32) Chen, R.; Bent, S. F. *Chem. Mater.* **2006**, *18*(16), 3733–3741.
(33) Aaltonen, T.; Ritala, M.; Sajavaara, T.; Keinonen, J.; Leskelä, M. *Chem. Mater.* **2003**, *15*, 1924–1928.
(34) Aaltonen, T.; Rahtu, A.; Ritala, M.; Leskela, M. *Electrochem. Solid-State Lett.* **2003**, *6*(9), C130–C133.

Table 1. Summary of the Ten Types of Samples Used in the Study[a]

sample	description	film thickness (nm)	Composition (%)			surface area (cm^2)
			Ru	Pt	O	
S1	ALD Pt:ALD Ru = 1:0	10.0	0.0	97.7	2.3	0.4071
S2	ALD Pt:ALD Ru = 8:4	10.2	12.3	86.9	1.8	0.8621
S3	ALD Pt:ALD Ru = 4:8	10.2	28.7	78.6	2.7	1.2821
S4	ALD Pt:ALD Ru = 4:16	10.8	50.8	46.3	2.9	1.3315
S5	ALD Pt:ALD Ru = 4:64	13.6	59.6	38.4	2.0	1.6427
S6	0 cycles of Pt ALD on sputtered Ru	0	100	0.0	0	2.4664
S7	10 cycles of Pt ALD on sputtered Ru	0.5	67.8	30.9	1.3	2.1303
S8	20 cycles of Pt ALD on sputtered Ru	1.0	48.3	50.0	1.7	2.6954
S9	30 cycles of Pt ALD on sputtered Ru	1.5	40.7	57.7	1.6	2.8081
S10	50 cycles of Pt ALD on sputtered Ru	2.5	0.0	97.4	2.6	0.9797

[a] Here, the Ru at.% and surface areas are derived from the XPS analysis and Cu-UPD analysis, respectively, on sample sets S1−S10. The Ru at.% value reported for each set is the average value obtained from 12 samples prepared in three different processes. The film thicknesses are estimates based on the experimentally determined ALD growth rates (~0.5 Å/cycle for Pt ALD and 0.2 Å/cycle Ru ALD). The film thickness is that of the ALD deposited films only; i.e., for the co-deposited films, it represents the total film thickness, whereas for the Pt skin catalysts, it represents only the ALD Pt skin. Samples S1−S5 are ALD co-deposited Pt−Ru catalysts. Samples S6−S10 are platinum overlayers of various thicknesses on sputtered ruthenium-coated FTO. For sample S6, the overlayer thickness is 0.

The ruthenium target material for sputtering was supplied by Kurt Lesker Co., with a purity of 99.99%. The sputtering chamber pressure was maintained at 1 Pa and sputtering was done at a power of 100 W. Subsequently, a Pt skin of specified thickness, controlled by the number of ALD cycles, was deposited onto the ruthenium-coated FTO substrates. Table 1 lists the specification of all of the Pt skin catalysts, with varying platinum loadings (samples S6−S10).

Catalyst Characterization. The film thickness was measured by ellipsometry (L116C He−Ne Ellipsometer, Gaertner Scientific Corporation) and X-ray reflectometry. A single-wavelength ellipsometer was used to measure metal thin films at thicknesses of < 5 nm. At larger thicknesses (> 5 nm), absorption becomes significant, which may lead to inaccurate measurements for this ellipsometer. For the X-ray reflection measurements, we used a PANalytical X'Pert PRO X-ray diffraction system to perform reflectometry analysis and obtain the film thickness. X-ray photoelectron spectroscopy (XPS) and scanning electron microscopy (SEM) were employed to investigate the composition and microstructure of the catalyst films. Scanning Auger electron spectroscopy (AES) was used to examine the dispersion of platinum and ruthenium over the substrates. The XPS system used here is an SSI S-probe monochromatized spectrometer, which uses Al Kα radiation (1486 eV) as a probe. All of the spectra shown in this paper have a detection sensitivity of ~0.1 at. %. All the SEM images presented in this paper were obtained in secondary electron mode. The instrument is a Model FEI XL30 Sirion SEM microscope with a field emission gun (FEG) source. Surface morphology was investigated by atomic force microscopy (AFM) (Digital Instruments, Inc., Santa Barbara, CA). The AES that we used was a PHI 700 Scanning Auger Nanoprobe that provides secondary electron image resolution down to 6 nm with the sample in the analytical position and an Auger resolution of 8 nm with high elemental sensitivity.

With a three-electrode cell, in which a platinum counter electrode and a Ag/AgCl reference electrode were used, electrochemical characterization (including cyclic voltammetry (CV) and chronoamperometry analysis (CA)) was performed on the catalysts at room temperature using a potentiostat from Bio-Logic SAS (SP-200). Methanol oxidation was used as the probe reaction in a 0.5 M H_2SO_4/16.6 M CH_3OH electrolyte solution, which was deaerated with N_2 for 20 min before electrochemical measurements. The surface area of each sample was determined by Cu underpotential deposition (Cu-UPD). All Cu-UPD experiments were conducted in a 0.002 M $CuSO_4$/0.1 M H_2SO_4 solution, unless otherwise stated. After electrochemical cleaning and transfer into a solution that contained dissolved cupric ions, the electrodes were held at 0.3 V for 180 s. A linear voltammetric scan was then performed from the admission potential to a point at which all of the Cu-UPD had been oxidized at a scan rate of 0.1 V/s. Current densities reported here are the measured currents normalized by the Cu-UPD-measured surface area of the sample.

Results and Discussion

ALD of Pt with $MeCpPtMe_3$ and O_2. Platinum thin-film deposition by ALD was initially studied by Aaltonen et al.,[33,34] using $MeCpPtMe_3$ and air or pure O_2 as precursors. Here, we employed the same precursors to prepare our platinum thin films by ALD. Figure 1a shows the growth curves for Pt ALD on ruthenium-coated silicon wafers and piranha-cleaned Si substrates at two different substrate temperatures: 245 and 295 °C. The platinum film thicknesses at cycle numbers of < 100 are consistently greater on the Ru substrates than on the SiO_2-coated Si substrates at both temperatures. Because these low cycle numbers correspond to the nucleation regime,[22,23,35] these results suggest that platinum nucleation occurs more readily on ruthenium than on SiO_2, which may explain why there is an abrupt change in the platinum growth rate on silicon substrates but not on ruthenium substrates. At higher cycle numbers, the growth rates on both substrates appear to approach the same value: ~0.5 Å/cycle. Figure 1b shows the effect of the precursor pulse times on the film growth rate. As the $MeCpPtMe_3$ pulse time is increased from 0.5 s, the growth rate slightly increases and saturates to 0.5 Å/cycle with pulse times of > 2.0 s. Saturation is also observed with O_2 pulse times longer than 1.0 s. This observation provides a reasonable verification of the self-limiting growth mechanism of the ALD Pt process.

The composition of the platinum films deposited by ALD was investigated by XPS. The XPS spectrum reveals

(35) Suntola, T. *Mater. Sci. Rep.* **1989**, *4*(5), 261.

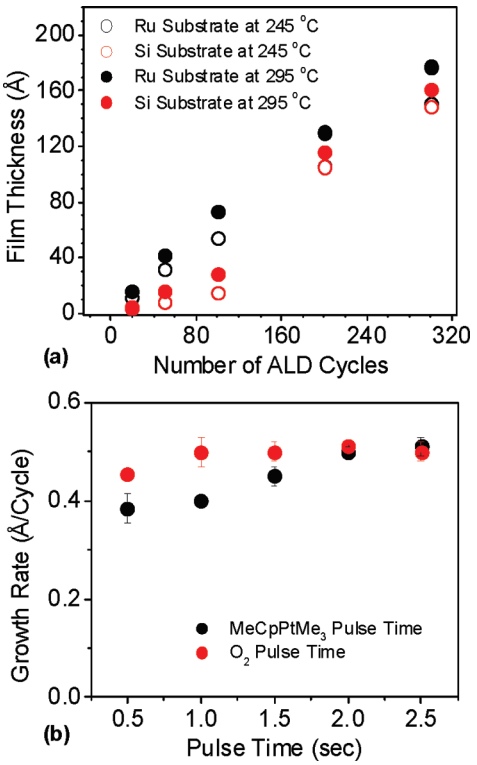

Figure 1. (a) Platinum growth curves on ruthenium and SiO_2 at 245 and 295 °C. (b) Dependence of the platinum film growth rate on the $MeCpPtMe_3$ and O_2 pulse times. Both the O_2 pulse time in the $MeCpPtMe_3$ experiments and the $MeCpPtMe_3$ pulse time in the O_2 pulse experiments were 2 s.

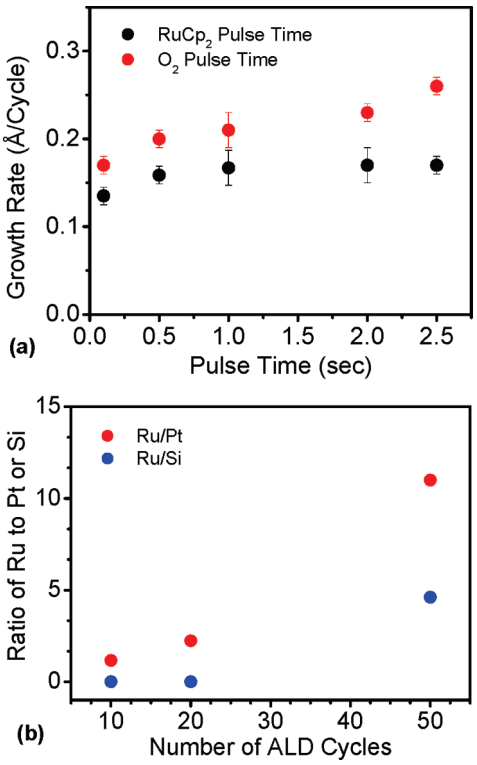

Figure 2. (a) Dependence of the ruthenium film growth rate on the $RuCp_2$ and O_2 pulse times at 245 °C; the O_2 pulse time in the $RuCp_2$ experiments was 0.1 s, and the $RuCp_2$ pulse time in the O_2 pulse experiments was 2 s. (b) Results of Ru ALD incubation time study on platinum- and SiO_2-coated silicon substrates at 245 °C showing the Ru signal versus the number of ALD cycles.

that the film, after sputtering off the topmost layers, is pure platinum, with no observable contaminants (to a sensitivity of 0.1 at. %). We have also used AFM to examine the surface morphology of the as-deposited platinum film. The root-mean-square (rms) film roughness of platinum thin films deposited on SiO_2/Si at 245 °C is ~1 nm, indicating that the as-deposited platinum films are very smooth for film thicknesses in the range of 1.2−15 nm (corresponding to 20−300 Pt ALD cycles). Across multiple samples, the rms roughness values varied, so caution must be used in reaching conclusions about any trends with thickness. However, a decrease in roughness at 300 cycles was reproducible across samples; this decrease may reflect coalescence of the islands formed in the initial nucleation process.[36,37] Generally, the roughness of these as-deposited platinum films is lower than that observed for films of the same thickness prepared using $MeCpPtMe_3$ and dry air;[38] the lower roughness may be a result of the reduced deposition temperature enabled by pure O_2.[39]

ALD of Ru with $Ru(Cp)_2$ and O_2. Ruthenium thin-film deposition by ALD has been studied by several groups, including Aaltonen et al.,[34] using $Ru(Cp)_2$ and air or pure O_2; Kim et al.,[40] using 2,4-(dimethylpentadienyl)(ethylcyclopentadienyl)Ru and O_2; and Han et al.,[41] using RuO_4 and H_2. In this study, we use $Ru(Cp)_2$ and pure O_2 because of its comparable deposition temperatures to that of the ALD Pt process and its relative ease to control the composition of the ruthenium thin films. We investigated the dependence of the ruthenium film growth rate on the $RuCp_2$ and O_2 pulse times at 245 °C. These data are shown in Figure 2a. As the $RuCp_2$ pulse time is increased from 0.1 s, the growth rate slightly increases and saturates at 0.17 Å/cycle for pulse times longer than 2.0 s. However, when we performed the same regimen for O_2 pulse times, we found the growth rate increased slightly from 0.17 Å/cycle to 0.26 Å/cycle when the O_2 pulse time increased from 0.1 s to 2.5 s. We believe that this occurs because longer O_2 pulse times lead to the formation of ruthenium oxide, which was also reported by Park et al.[42] Our elemental analysis data (vide infra) confirms this hypothesis. A separate incubation time study of Ru ALD on Pt and SiO_2/Si substrates performed for lower numbers of cycles, shown in Figure 2b, indicates that ruthenium nucleates better on platinum, compared to nucleation onto silicon oxide-coated silicon, with consistently more ruthenium deposited on the platinum surface than on the

(36) Maissel, L. I.; Glang, R. *Handbook of Thin-Film Technology*; McGraw−Hill: New York, 1970.
(37) Nayak, M.; Ezhilvalavan, S.; Tseng, T. Y. *Handbook of Thin Film Materials*; Academic Press: San Diego, CA, 2001; Vol. *3*, p 121.
(38) Jiang, X.; Huang, H.; Prinz, F. B.; Bent, S. F. *Chem. Mater.* **2008**, *20*(12), 3897–3905.
(39) Aaltonen, T.; Ritala, M.; Tung, Y. L.; Chi, Y.; Arstila, K.; Meinander, K.; Leskela, M. *J. Mater. Res.* **2004**, *19*, 3353.
(40) Kim, S. K. L.; Y., S.; Lee, S. W.; Hwang, G. W.; Hwang, C. S.; Lee, J. W.; Jeong *J. Electrochem. Soc.* **2007**, *154*, D95–D101.
(41) Han, J. H. L.; S., W.; Choi, G.-J.; Lee, S. Y.; Hwang, C. S.; Dussarrat, C.; Gatineau, J. *Chem. Mater.* **2008**, *21*, 207.
(42) Park, K. J.; Doub, J. M.; Gougousi, T.; Parsons, G. N. *Appl. Phys. Lett.* **2005**, 86.

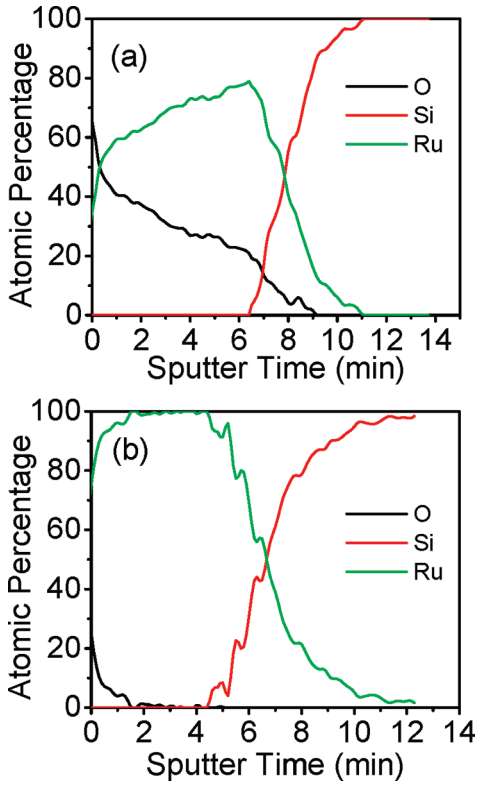

Figure 3. AES depth profiles of two as-deposited ruthenium films deposited with pulse times of (a) 2 s and (b) 0.1 s on silicon at 245 °C.

silicon substrate. Therefore, for our Pt−Ru co-deposition process for catalyst application, we predeposit a thin layer of platinum on the FTO substrates to assist nucleation.

It is interesting to note that both platinum and ruthenium prefer to nucleate on metal substrates and less so on an insulating silicon substrate. We do not fully understand the origin of this difference, but it appears that the substrate properties play a critical role in these systems. It would be interesting to perform an in situ study to investigate the mechanism of both platinum and ruthenium nucleation on these different substrates.

After investigation of the ruthenium growth curves, we examined the composition of the ruthenium films deposited with different oxygen pulse times using AES depth profiling. Figure 3 shows the depth profiles of three elements, including oxygen, silicon, and ruthenium for two different as-deposited Ru samples: ruthenium films fabricated with an oxygen pulse time of 2 s (Figure 3a) and ruthenium films fabricated with an oxygen pulse time of 0.1 s (Figure 3b). The depth profiles show that oxygen is present at the film surface as well as within the film when the oxygen pulse length is 2 s (see Figure 3a), although the amount of oxygen decreases with distance from the surface. This oxygen may come from a combination of surface contamination and the film deposition process itself, particularly if there is an excess of oxygen in the reactor. When the O_2 pulse time is decreased to 0.1 s (Figure 3b), the AES depth profile indicates that oxygen is limited to the film surface and is not present in the bulk ruthenium film. The surface oxygen in this case likely arises from surface contamination. Based on the results of

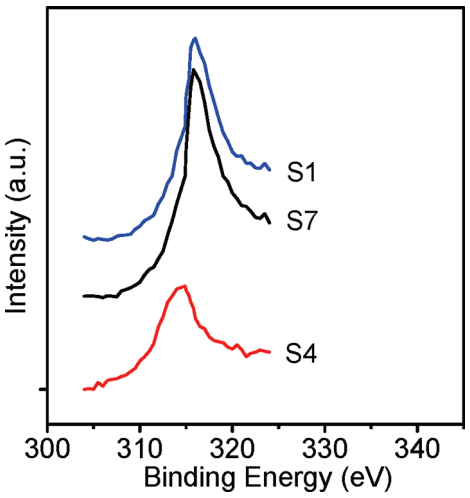

Figure 4. High-resolution XPS scans of Pt $4d_5$ peaks of samples S1, S4, and S7.

the AES depth analysis, subsequent co-deposition processes were performed using an O_2 dose time of 1 s, because it leads to the growth of metallic ruthenium films and avoids the deposition of RuO_x.

In addition to the film composition analysis, we also investigated the ruthenium film morphology using AFM. Compared to platinum films of the same thickness, the ALD Ru film are much rougher. The rms roughness of a 5-nm film, deposited in 400 cycles, is ~4.2 nm, compared to an rms roughness of ~1 nm for platinum.

Physical Characterization of the Co-deposited Pt−Ru Catalysts and Pt Skin Catalysts. The properties and the fabrication conditions of the co-deposited Pt−Ru catalysts and Pt skin catalysts are listed in Table 1. The composition values in Table 1 were obtained by XPS, so they are most indicative of surface compositions. For the co-deposited catalysts (samples S1−S5), the ruthenium content increases as the relative number of Ru cycles is increased in each process, with the resulting ruthenium content varying from 0 at. % to 59.6 at. %. For the Pt skin catalysts (samples S6−S10), the XPS-measured ruthenium content progressively decreases as the number of Pt ALD cycles increases, from sample S6, which is pure ruthenium without an ALD Pt coating, to sample S10, taken after 50 cycles of Pt ALD. The XPS-measured Ru signal or nominal ruthenium content is completely masked by the platinum overlayer deposited in 50 cycles. The nominal ruthenium content measured by XPS is between 100 at. % and 0 at. % for samples S6−S10. In addition to the composition analysis, XPS was also employed to probe the chemical shift of all catalysts. High-resolution XPS scans of Pt $4d_5$ peaks of samples S1, S4, and S7 are shown in Figure 4, which demonstrate that the Pt $4d_5$ peaks of both samples S4 and S7 are red-shifted, compared to that of sample S1. This occurs because platinum has slightly larger electronegativity compared to ruthenium, and Ru d electrons are more readily transferred to Pt.[43] The impact of this electronic effect

(43) Nøskov, J. K.; Lang, N. D. *Phys. Rev. B* **1980**, *21*(6), 2131.

Figure 5. SEM image (left) and AES elemental mapping of Ru and Pt (middle and right), respectively, of sample S4.

is observed to be more significant on sample S4, compared to that of sample S7.

SEM analysis was used to examine the microstructure of the Pt−Ru catalysts (see the Supporting Information). The major morphological features of these catalysts (samples S1−S5) reflect those of the FTO-coated glass substrate itself, which is what we expect, because of the high conformality of the ALD films. Sample S6 is sputtered ruthenium on FTO, which forms a cauliflower-like morphology overlaying the FTO grains. The major morphology of these catalysts resembles sample S6, the sputtered ruthenium-coated FTO, again because of the high conformality of the ALD-deposited Pt overlayers.

We also performed AES analysis on sample S4, which was prepared through ALD co-deposition, and on sample S7, which was sputtered ruthenium coated with a thin ALD Pt overlayer, because of their unusual electrochemical behavior, as discussed later. The results of AES survey scans show that the nominal surface compositions of samples S4 and S7 are $Ru_{0.50}Pt_{0.46}O_{0.04}$ and $Ru_{0.68}Pt_{0.31}O_{0.01}$, respectively. These surface compositions are in good agreement with the XPS results shown in Table 1.

Auger elemental mapping of Pt and Ru of both samples illustrates that the dispersion of platinum and ruthenium over the substrate is relatively uniform. For example, AES elemental mappings of both Ru and Pt of sample S4 are shown in the middle and right columns, respectively, of Figure 5. The AES mapping of the Pt signal in sample S7 (not shown) is similar but appears to be more particulate. The particle-like morphology of the platinum in sample S7 is attributed to its low film thickness: with 10 ALD cycles corresponding to only ~5 Å of platinum, the deposition is still in the nucleation stage and the platinum has not yet coalesced into a continuous film. The uniform dispersion can be understood by the thermodynamics of the film deposition process.[44] Calculations based on enthalpies of atomization show that the surface free energy of Pt (2.7 J/m^2) is lower than that of Ru (3.4 J/m^2).[45,46] Thus, in the ALD of Pt on Ru, the platinum film tends to wet the ruthenium substrate to minimize the total free energy, leading to a good degree of coating of platinum on ruthenium.

Considering the differences in surface morphology between the different Pt−Ru catalysts, an appropriate measurement of the surface area is necessary to compare the electrochemical catalytic activity of these catalysts. To quantify the total areas of Pt and Ru surface sites for all of the catalysts, we have used Cu underpotential deposition (Cu-UPD), which is a viable and reliable method, as previously demonstrated by Green and Kucernak.[47] The charges for copper stripping were determined by integrating the curves in the potential region of 0.3−0.8 V vs RHE and dividing them by the scan rate (0.1 V/s); the total surface areas of platinum and ruthenium were then calculated by dividing by the charge associated with the following reaction, which is 420 μC/cm^2.

$$Cu^{2+} + 2e^- \leftrightarrow Cu_{upd}$$

The copper stripping curves were background-subtracted prior to integration; i.e., the current from the cyclic voltammogram obtained in 0.1 M H_2SO_4 was subtracted from the copper-stripping voltammograms for all the samples. The surface areas of the various Pt−Ru catalysts determined by the copper-stripping method are presented in Table 1. The currents in all the electrochemical experiments that follow are normalized to the respective active platinum and ruthenium surface areas.

Electrochemical Behavior of ALD Pt−Ru Catalysts and Pt Skin Catalysts. After physical characterization, the electrochemical behavior of the co-deposited Pt−Ru catalysts and the Pt skin catalysts was examined for methanol oxidation using cyclic voltammetry (CV), to systematically compare catalytic activity and onset of methanol oxidation, and by chronoamperometry (CA), to determine the stability and performance of these prospective catalytic anodes. For CV measurements, we started the voltage sweep in the anodic direction from an initial potential of 0 V and cycled the potential of each Pt−Ru catalyst multiple times between 0 V and 0.8 V at a scan rate of 0.1 V/s in two different solutions: 0.5 M H_2SO_4 as a background control, and a concentrated methanol solution of 16.6 M CH_3OH/0.5 M H_2SO_4 to investigate the induced oxidation current, which is a key parameter that positively correlates to the catalyst activity.

Figure 6 shows the anodic scans of the CV measurements in solutions both with and without methanol, traced by solid lines and dashed lines, respectively. The difference from these curves is the induced current from methanol oxidation. A better catalyst is characterized by a higher induced current density at a given applied potential or a lower onset potential. For the co-deposited Pt−Ru catalysts (samples S1−S5), the data clearly illustrate that the catalyst activity, indicated by the induced current density at ~0.6 V, increases when the ruthenium content increases, and reaches a maximum value when the ruthenium content reaches 51% (sample S4), before dropping off when the ruthenium content increases further. Moreover, all of the ruthenium-containing catalysts (samples S2−S5, where the ruthenium content is in the range of 12.3−59.6 at. %) exhibit higher activities compared to pure platinum. The enhancement can be explained by the bifunctional mechanism, where ruthenium dehydrogenates water at a much lower potential

(44) Wuttig, M.; Liu, X. *Ultrathin Metal Films: Magnetic and Structural Properties*, 1st ed.; Springer: Berlin, 2005; p 9.
(45) Hara, S.; Izumi, S.; Kumagai, T.; Sakai, S. *Surf. Sci.* **2005**, *585* (1−2), 17.
(46) Eaglesham, D. J.; White, A. E.; Feldman, L. C.; Moriya, N.; Jacobson, D. C. *Phys. Rev. Lett.* **1993**, *70*(11), 1643.
(47) Green, C. L.; Kucernak, A. *J. Phys. Chem. B* **2002**, *106*, 11446.

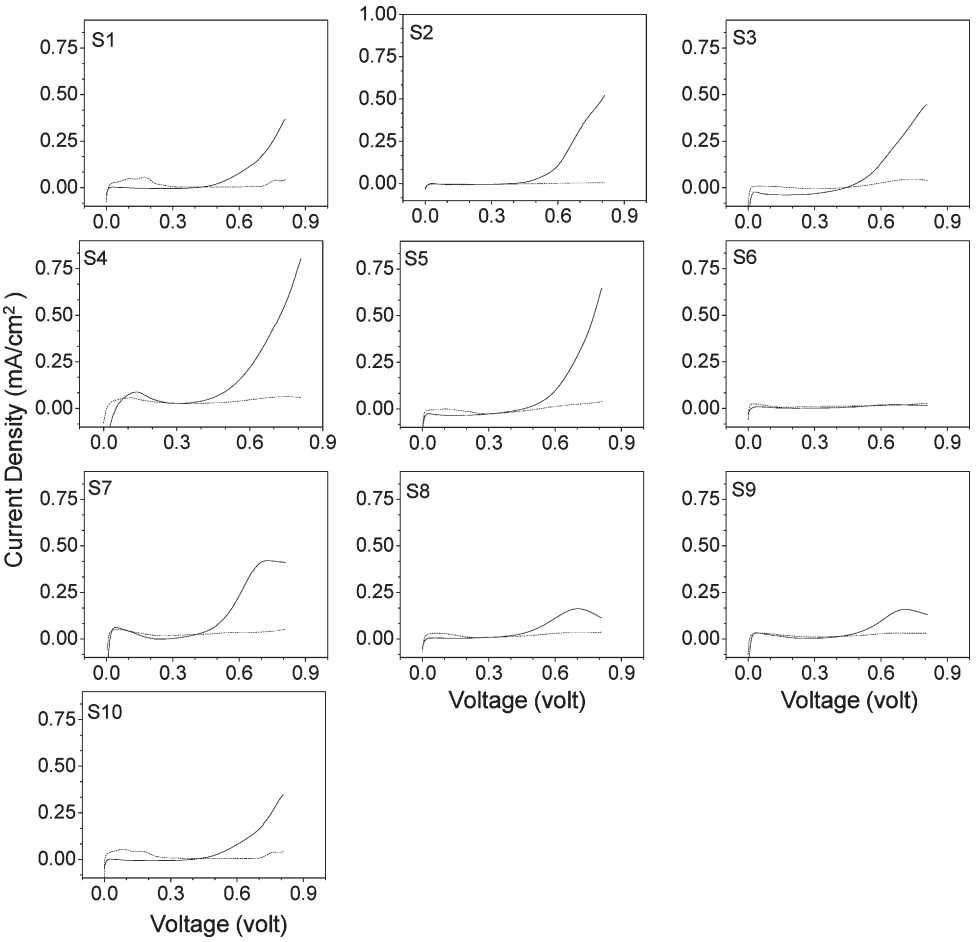

Figure 6. Cyclic voltammograms of ALD co-deposited Pt−Ru catalysts (samples S1−S5) and Pt skin catalysts (samples S6−S10) in 16.6 M CH_3OH/0.5 M H_2SO_4 (solid line) at a scan rate of 0.1 V/s. Background voltammograms in 0.5 M H_2SO_4 are shown as dashed lines.

(0.2 V vs RHE) and facilitates the removal of CO intermediates, which are strongly adsorbed on the Pt active sites.[6,8,48] Therefore, the presence of some ruthenium enhances the overall methanol oxidation kinetics compared to pure platinum. Among samples S1−S5, sample S4 also showed the minimum onset potential for methanol oxidation.

Sample S6, the sputtered ruthenium film, shows negligible methanol oxidation current. This result is expected, because ruthenium is an inactive catalyst material for methanol oxidation, as reported in the literature.[8] For the sputtered ruthenium samples with a platinum overlayer (samples S7−S10), the methanol-oxidation-induced current densities, corresponding to their catalytic activities, decrease as the platinum loading increases, with sample S7 being the most active catalyst. Sample S10 exhibits current densities that are comparable to that of sample S1, which is pure platinum, as characterized by XPS. The Pt skin catalyst results can be explained as follows. According to theory, for a very thin platinum overlayer, the underlying ruthenium films are able to weaken the bonds between the methanol oxidation intermediates and platinum, leading to enhanced catalytic activity, even compared to pure platinum.[26−28] However, the impact of the ruthenium underlayer is expected to decrease as the thickness of the platinum overlayer increases. When the platinum skin is too thick, the impact of the ruthenium underlayer becomes negligible. Accordingly, the thinner platinum overlayer (sample S7, with ~5 Å of platinum) has superior catalytic activity among all of the Pt skin catalysts of various thicknesses.

To study the time-dependent behavior of the Pt−Ru catalysts toward methanol oxidation, CA experiments were performed. The inset in Figure 7a is the CA analysis for 900 min on all of the catalysts measured in 16.6 M CH_3OH/0.5 M H_2SO_4 at 0.6 V vs RHE, which represents the onset potential of methanol oxidation on pure platinum. The performance of all of the samples is observed to degrade within this time scale. That of samples S1 and S10 (pure platinum) decreases more rapidly than the other catalysts, because of the poisoning by intermediates.[2,7−9] Sample S6 (pure ruthenium) exhibits a negligible induced methanol oxidation density, as explained above. Among all the catalysts, sample S4 (50.8% ruthenium) demonstrates the highest methanol oxidation current at t = 900 min, followed by samples S3 (28.7% ruthenium), S7 (67.8% ruthenium), S2 (12.3% ruthenium), S5 (59.6% ruthenium), and then samples S8 (48.3% ruthenium), S9 (40.7% ruthenium), S1 (0% ruthenium), and S10 (0% ruthenium). The higher activity

(48) Roth, C.; Martz, N.; Hahn, F.; Leger, J. M.; Lamy, C.; Fuess, H. *J. Electrochem. Soc.* **2002**, *149*(11), E433–E439.

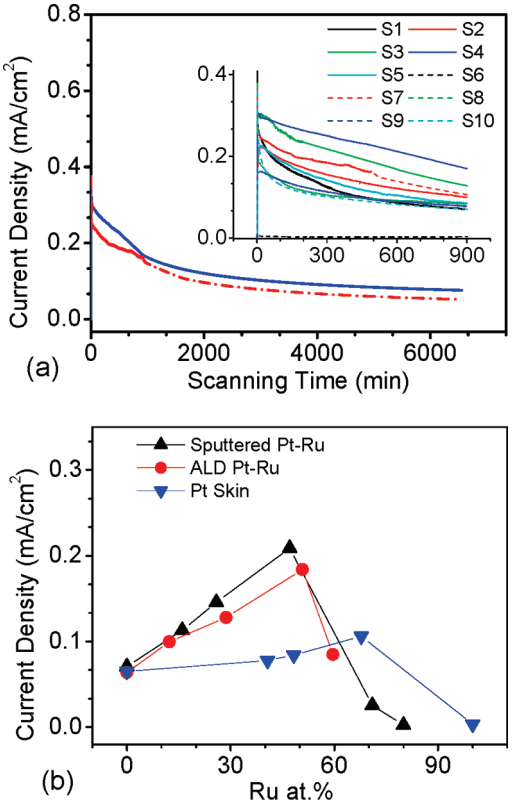

Figure 7. (a) Chronoamperometry (CA) analysis of samples S4 and S7 up to 6550 min in 16.6 M CH_3OH/0.5 M H_2SO_4 at 0.6 V vs RHE. (b) Methanol oxidation activity plots, extracted from CA curves of co-sputtered Pt−Ru catalysts[16] (data denoted by upright solid triangles), ALD co-deposited Pt−Ru catalysts (data denoted by solid circles), and the Pt skin catalysts (data denoted by inverted solid triangles), as a function of the ruthenium composition measured in 16.6 CH_3OH/0.5 M H_2SO_4, at 0.6 V vs RHE at t = 900 min. The inset in panel (a) is the CA analysis of samples S1−S10 up to 900 min; the x-axis and y-axis titles are "scanning time (min)" and "current density (mA/cm^2)", respectively.

in the mixed Pt−Ru catalysts can be attributed to the bifunctional mechanism, in which the Ru atoms, in the proximity of Pt atoms, form surface oxides at potentials much lower than on platinum and provide local oxygen to oxidize and desorb the poisonous intermediates on active Pt sites.[8,49] In addition, an electronic effect may also play a role here. As mentioned earlier, our XPS study indicated that the Pt $4d_5$ peak shifts to lower energy when the ruthenium content increases, because of the transfer of Ru d electrons onto Pt. In the methanol oxidation process, this will cause polarization of the Pt−Ru bonds in the alloys and weaken the Pt−CO bond. The electronic effect on sample S4 is more significant than that on sample S7, according to the change in the Pt $4d_5$ peaks (in comparison).

To test the catalyst stability at prolonged times, CA experiments were performed on both samples S4 (50.8% ruthenium) and S7 (67.8% ruthenium), representing the most active co-deposited catalyst and Pt skin catalyst, respectively, in 16.6 M CH_3OH/0.5 M H_2SO_4 at 0.6 V vs RHE for up to 6600 min (or 110 h). Figure 7a shows the corresponding CA curves, in which the current densities decrease very quickly at the beginning and level off after ~4000 min. The measured current densities at t = 6600 min are 0.07605 mA/cm^2 for sample S4 (50.8% ruthenium) and 0.05001 mA/cm^2 for sample S7 (67.8% ruthenium). These values are comparable to other methanol oxidation catalysts under the same concentration and conditions. For example, our previous studies on sputter-deposited Pt−Ru films showed that the best two catalysts among the sputtered Pt−Ru catalysts have compositions of 47.1% ruthenium and 25.9% ruthenium.[16] Their corresponding current densities, measured at t = 6600 min, were 0.06934 mA/cm^2 and 0.05605 mA/cm^2, respectively, which are values similar to those measured here. Moreover, the current densities for the ALD co-deposited Pt−Ru catalysts compare well with that of pure sputtered platinum, which is 0.07056 mA/cm^2, measured at much earlier times (900 min; see the inset of Figure 7a), suggesting comparable catalytic activity. While the ALD-fabricated Pt skin catalysts are not as active as the co-deposited samples, note that they are able to deliver reasonable activity after coating a platinum overlayer as thin as 5 Å, suggesting that they provide an effective and efficient way of increasing utilization while reducing the loading of platinum. Figure 7b summarizes, for the Pt−Ru system, as a function of the ruthenium composition, the methanol oxidation activity, which is characterized by the current density at the end of 900 min for CA measurements performed in 16.6 CH_3OH/0.5 M H_2SO_4. Results of a previous study on co-sputtered Pt−Ru films are also included in Figure 7b for comparison.[16] For both ALD co-deposited Pt−Ru catalysts and co-sputtered Pt−Ru catalysts, the highest catalytic activity is achieved when the ruthenium content is ~50% (sample S4), which is consistent with the majority of literature reports.[6,10−14,50−57] Moreover, the current densities of the catalysts prepared by either ALD co-deposition or co-sputtering are comparable at 900 min for each of the compositions studied. Somewhat different behavior is observed for the Pt skin catalysts. For the Pt skin catalysts, the highest current density is achieved for sample S7 (which has a ruthenium content of 68 at. %), for which the estimated platinum overlayer thickness is 5 Å. When the platinum overlayers become thicker (shown as smaller ruthenium contents (in terms of at. %) in Figure 7b), the ability of the ruthenium to influence the electronic structure of the platinum is expected to be reduced, according to the theoretical predictions.[26] However, because the ALD Pt skin likely is not continuous for

(49) Lu, C.; Rice, C.; Masel, R. I.; Babu, P. K.; Waszczuk, P.; Kim, H. S.; Oldfield, E.; Wieckowski, A. *J. Phys. Chem. B* **2002**, *106*(37), 9581–9589.
(50) Tang, Z. C.; Lu, G. X. *Progress Chem.* **2007**, *19*(9), 1301.
(51) Arico, A. S.; Antonucci, P. L.; Modica, E.; Baglio, V.; Kim, H.; Antonucci, V. *Electrochim. Acta* **2002**, *47*(22−23), 3723.
(52) Choi, W. C.; Jeon, M. K.; Kim, Y. J.; Woo, S. I.; Hong, W. H. *Catal. Today* **2004**, *93*−*95*, 517.
(53) Xue, X.; Lu, T.; Liu, C.; Xu, W.; Su, Y.; Lv, Y.; Xing, W. *Electrochim. Acta* **2005**, *50*(16−17), 3470.
(54) Baldauf, M.; Preidel, W. *J. Power Sources* **1999**, *84*(2), 161.
(55) Du, J.; Yuan, X. X.; Chao, Y. J.; Ma, Z. F. *Rare Met. Mater. Eng.* **2007**, *36*(7), 1309.
(56) Xu, M.; Zhang, Z.; Yang, X. *J. Funct. Mater.* **2006**, *37*, 419.
(57) Antolini, E. *Mater. Chem. Phys.* **2003**, *78*(3), 563.

lower numbers of ALD cycles, exposing both platinum and ruthenium to the electrolyte solution, the formal core−shell catalyst model may not apply for the thinner skin layers. Nevertheless, the trend as observed in Figure 7b does show a decrease with platinum thickness. Several other observations can be made. First, even at the peak, the activity of the Pt skin catalysts studied in this work is not as good as that of the catalysts prepared using the other two approaches. Second, the activity of ruthenium with a thin platinum layer does exceed the activity for pure platinum, confirming the synergistic effect between platinum and ruthenium.

Conclusions

In our atomic layer deposition (ALD) studies, we observed that both platinum and ruthenium prefer to nucleate on metal substrates than on silicon oxide-covered silicon substrates. An in situ study on the nucleation mechanism of ALD Pt and ALD Ru on these different substrates is desirable for future research.

The electrochemical studies in concentrated methanol solution show that the optimal stoichiometric Pt:Ru ratio is ~1:1 for the co-deposited Pt−Ru catalysts. However, for the Pt skin catalysts, the optimal activity is achieved for sample S7, which has a ruthenium content of 67.8 at. %, corresponding to a 5-Å-thick platinum overlayer, the performance of which is comparable to that of sample S2, which is the co-deposited sample with a ruthenium content of 12.3 at. %. This may be because of porosity in the platinum overlayer which exposes the underlying ruthenium. Therefore, the Pt skin catalyst may behave like a co-deposited catalyst when the platinum overlayer is thin enough, which also explains the dependence of activity of the skin catalysts on the platinum thickness and is consistent with the skin catalyst model. In summary, the catalytic activity observed for the ALD co-deposited Pt−Ru catalysts is comparable to that of sputtered Pt−Ru catalysts, while the Pt skin catalysts show only moderately reduced activity achieved with a platinum overlayer as thin as 5 Å. This result shows that ALD is a promising technique for preparing catalysts of enhanced activity compared to pure platinum with very small loadings of platinum.

Typically, catalytic activity increases as temperature increases. Our plan for follow-up study will be to characterize the electrochemical behavior of sputtered Pt−Ru catalysts in stoichiometric steam/methanol mixtures at elevated temperatures. It will be interesting to study the long-term (> 110 h) stability of the catalysts' electrochemical behavior, and the change of the morphology and surface composition of such nanostructures over time. In addition, high-resolution structural characterization, such as transmission electron microscopy, will be very appealing to reveal the structure of the Pt skin catalysts studied here.

Acknowledgment. The authors thank the DMFC Industrial Consortium at Stanford for financial assistance and Prof. Thomas F. Jaramillo for helpful discussions and generously offering the use of his group's potentiostat.

Supporting Information Available: Plan-view AFM images of Pt thin films and Ru thin films deposited on SiO_2/Si substrates at at 245 °C. SEM images of the co-deposited Pt−Ru catalysts and Pt skin catalysts. Cu-UPD experiments on co-deposited Pt−Ru catalysts and Pt skin catalysts. Cyclic voltammograms of Pt−Ru samples in 0.5 M H_2SO_4 obtained at a scan rate of 0.1 V/s. This information is available free of charge via the Internet at http://pubs.acs.org.